Supplementary Information

Na-PHYTATE DECOMPOSITION BY AEROBIC SOIL MICROORGANISMS: PHOSPHATE RELEASE AND SPECTROMETRIC INDEXING OF PHYTASE EFFICIENCY

Nadiia Yamborko [1,2,3], Hryhoriy Stryhanyuk [2*], Peter Herzsprung [4], Julia Becker-Jahn [5], Jan Griebel [5], Wolf von Tümpling [6], Galyna O. Iutynska [3], Evgenia V. Blagodatskaya [1]

[1] *Department of Soil Ecology, Helmholtz Centre for Environmental Research – UFZ, Theodor-Lieser-Straße 4, 06120 Halle, Germany*

[2] *Department of Technical Biogeochemistry, Helmholtz Centre for Environmental Research – UFZ, Permoserstraße 15, 04318 Leipzig, Germany*

[3] *Department of General and Soil Microbiology, Zabolotny Institute of Microbiology and Virology, NASU, Akademika Zabolotnoho Str. 154, 03143 Kyiv, Ukraine*

[4] *Department of Lake Research, Helmholtz Center for Environmental Research – UFZ, Brückstraße 3a, 39114 Magdeburg, Germany*

[5] *Leibniz Institute of Surface Engineering (IOM), Permoserstraße 15, 04318 Leipzig, Germany*

[6] *Department of River Ecology, Helmholtz Center for Environmental Research – UFZ, Brückstraße 3a, 39114 Magdeburg, Germany*

**Correspondence:* gregory.stryhanyuk@ufz.de

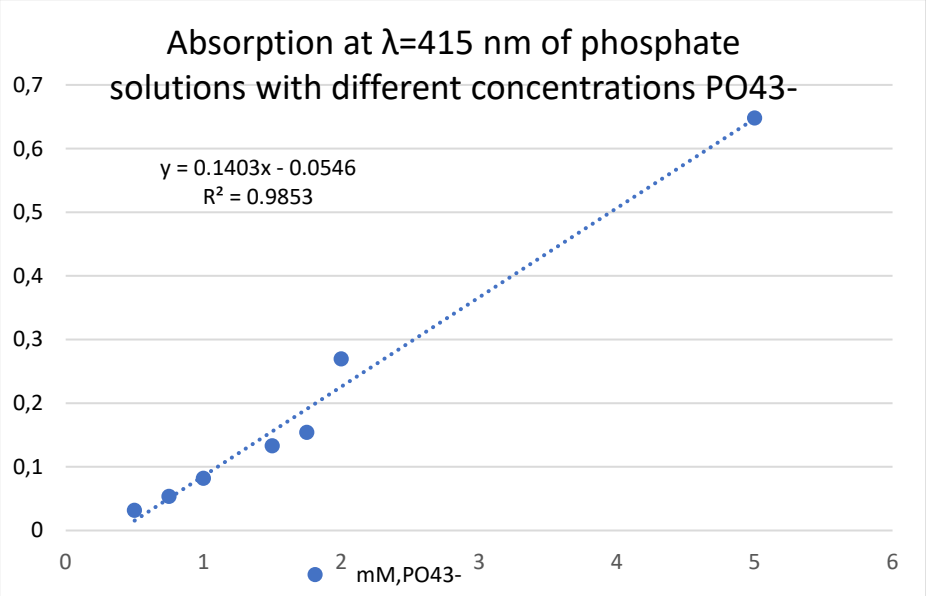

Figure S1: Calibration curve: OD dependence (optical density) from phosphate ion content (mM) in water solution.

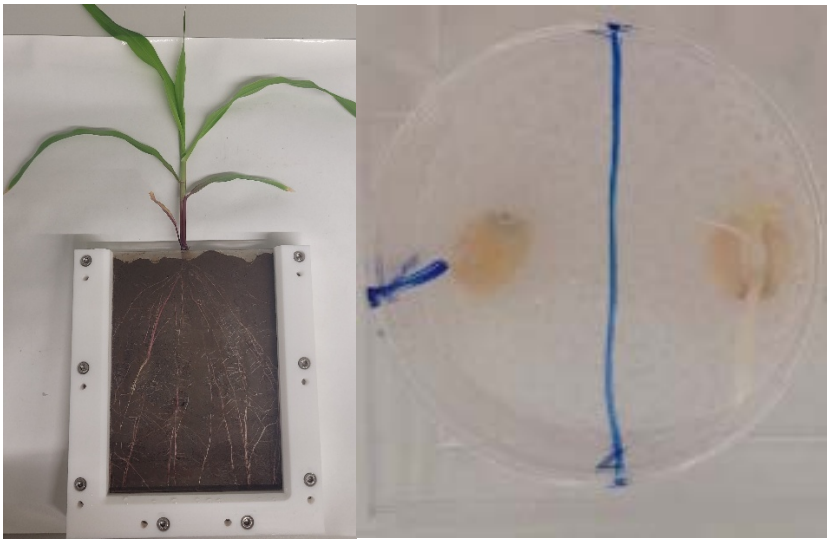

Figure S2: Germination of seeds and rhizobox cultivation.

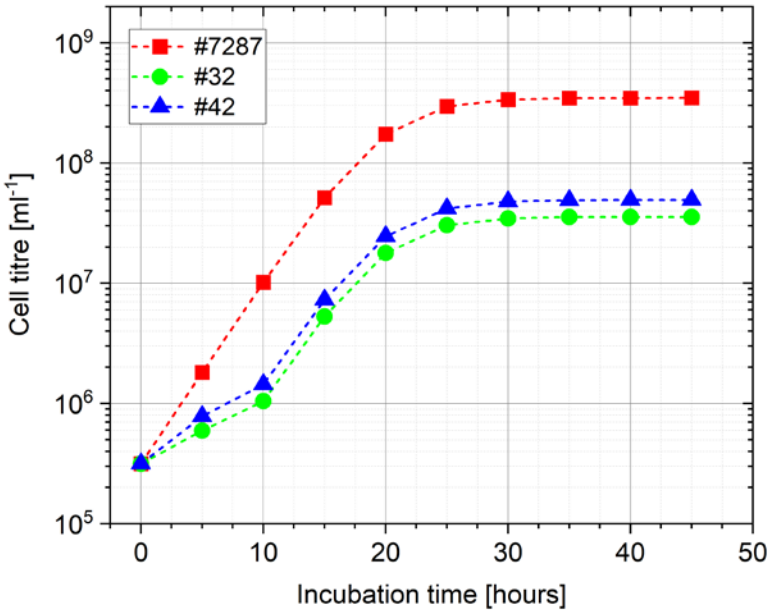

Figure S3: Growth curves for soil microbial strains cultivated on 8 mM Na-phytate as a sole phosphorus and carbon substrate at 28°C.

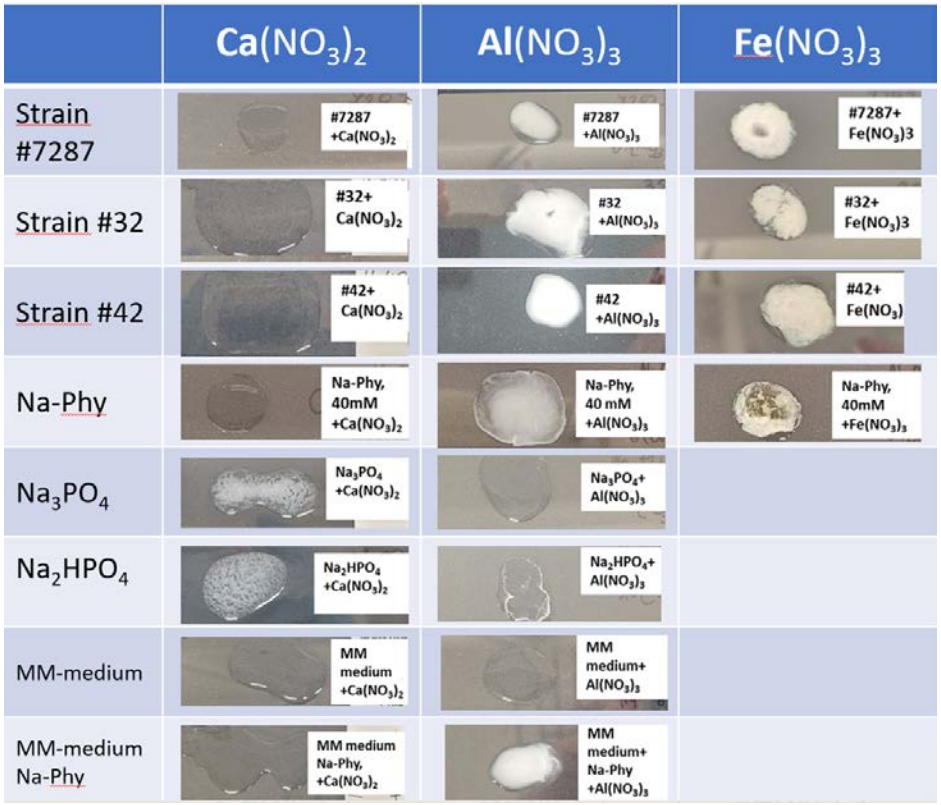

Figure S4: Precipitation reactions of Ca^{2+}, Al^{3+} and Fe^{3+} nitrate solutes with mineral and organic Na-Phy phosphates.

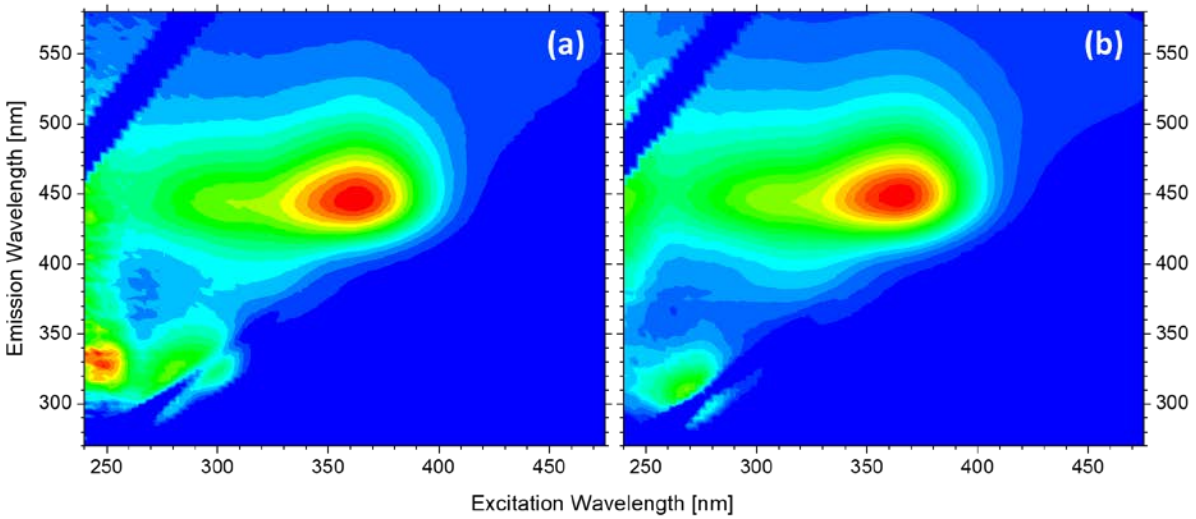

Figure S5: Development of photoluminescence spectra of 10mM Na-phytate solution. Frame (a) – fresh solution; frame (b) – after 1 month storage at room temperature.

UV-absorption spectroscopy

Considering the impact of thermal treatment and storage on fluorescence spectra from Na-Phy solution, considerable part of spectroscopic investigation of phytate decomposition was based on UV-absorption spectroscopy to study the phytate energy-states relaxing non-radiatively i.e. without emitting fluorescence photons.

UV-absorption spectra of Na-Phy reveal the interactions of the phosphate groups and the inositol ring with UV light [1]. The presence of metal ions stabilizing the phosphate ligands cause the Ligand-to-Metal Charge Transfer (LMCT) transitions (i.e., electrons transfer from the phosphate ligand to metal ion) contributing to UV-absorption spectrum of phytates [2, 3]. The efficiency of this transfer depends on the metal's electron affinity and the orbital overlap with the ligand. The exact spectral range of absorption depends on the type of metal ion and the experimental conditions [1]. Sodium phytate dissociates in water, releasing sodium ions and forming highly charged phytate anions. The ionic interaction of the dissociation products is revealed in the UV-absorption and luminescence properties. Na-Phy dissociation enhances solubility and the availability of negatively charged phosphate groups, but it does not introduce new chromophores [4]. Na-phytate has been proved not to form any complexes, but the revealed increase in their UV absorption was assigned to thermal impact [5].

Figure S6a shows the difference in absorption spectra of cold and autoclaved Na-phy solutions. The fresh Na-Phy reveals 3 broad absorption bands with maxima around 275 nm, 218 nm and 191 nm (Fig. S6a, blue).

The UV-absorbance of Na-phytate increases considerably after autoclaving and has been measured without saturation after 16x dilution (Fig. S6a, red) revealing a complex absorption band within 190-245 nm with the main sharp peak at 217 nm. Intensified absorption of autoclaved Na-Phy solution below 250 nm may be caused by the release of orthophosphate anions upon thermal destruction of Na-Phy molecules. The absorption of Na-Phy below 250 nm may be also related to the interactions involving phytate inositol-rings via the interplay of electrostatic forces with or between molecular sites of different electron density, e.g. highly-dense π-electron cloud with one stronger hybridized and revealing therefore less local electron density [6]. Alternatively, non-destructive sterilization of Na-Phy solutions might be possible via microwave treatment (see Fig. S7), but the elucidation of its application efficiency requires further investigations.

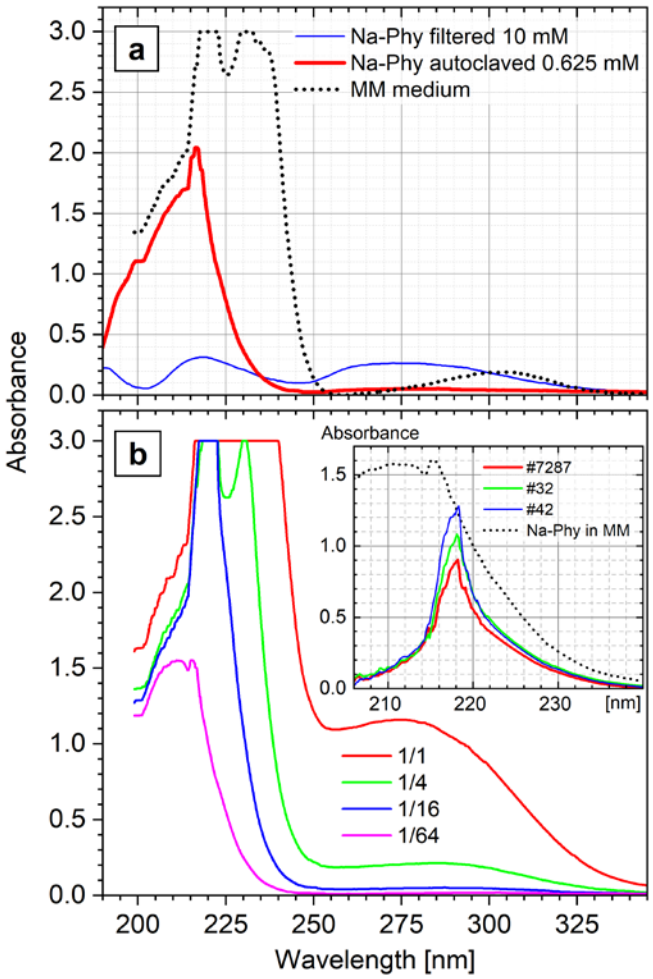

Figure S6: Frame a shows the absorption spectra of freshly prepared (blue) and autoclaved (red) 10 mM Na-Phy solution diluted 16x to 0.625 mM together with the absorption of non-diluted MM medium (dotted black). Frame b: absorption of mineral medium with initial 32 mM Na-Phy at different dilution degrees. The inset in frame b represents the absorption of 64x diluted supernatant culture liquids (coloured solid) after the subtraction of corresponding mineral medium contribution (black dotted).

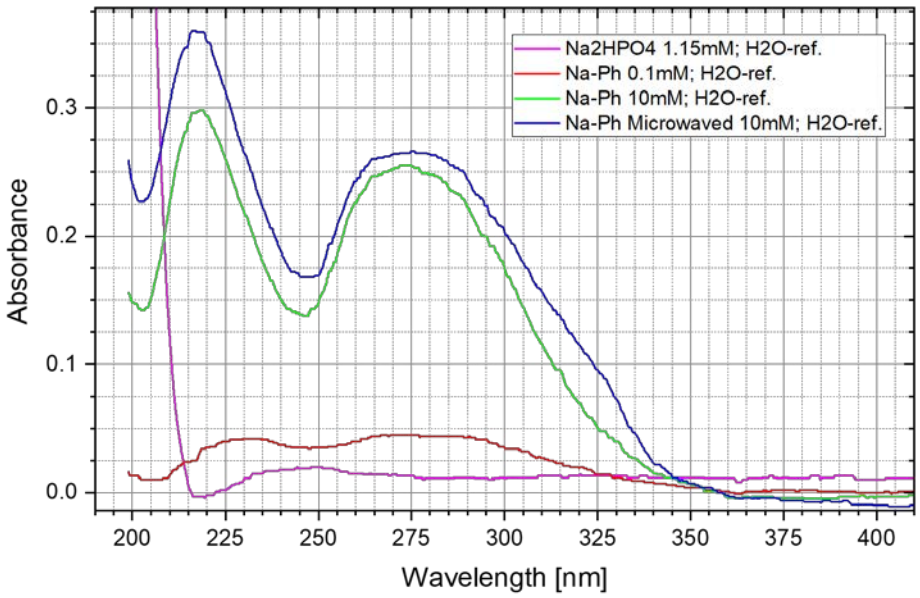

Figure S7: Absorption spectra of "cold" (green), microwaved (blue) 10 mM Na-phytate solution in water, "cold" 0.1 mM Na-phytate (red) and Na_2HPO_4 1.15 mM absorption (magenta).

Biotic conversion of Na-phytate as carbon and phosphorus source upon microbial cultivation

The MM medium without Na-Phy introduces the new absorption band at 305 nm and the intensive absorption continuum with 250 nm onset (Fig. S6a, black dotted) additionally to the absorption of filtrated Na-Phy. The energy of ionic group absorption, i.e. position of corresponding absorption band, vary in combination of different cation-anion groups. The complex absorption profile below 250 nm reveals the interaction in groups of SO_4^{2-}, NO_3^-, Cl^-, and Mg^{2+}, Na^+, K^+ ions in the MM medium. Dilution of Na-Phy in MM-medium causes the considerable reduction of low-energy absorption components (Fig. S6b) confirming their relation with the intermolecular ligand interaction.

The absorption in the narrow 217 nm peak is well pronounced for the diluted Na-Phy solution in MM-medium (Fig. S6b, magenta) and its intensity reveals the major difference in the absorption of the supernatant culture liquids (Fig. S8) after growth of 3 phytase-active bacterial strains with 32 mM Na-Phy provided as an exclusive carbon and phosphorus source. To eliminate the absorption by mineral medium component, its absorption spectrum at highest 64x dilution was subtracted from the corresponding absorption spectra of culture liquids. The resulted supernatant absorption spectra after medium-background subtraction are presented in the inset of Fig. S6b with coloured solid lines. With the phytase efficiency decreasing in [#7287, #32, #42] strain series (see Fig. 3 in the main text) the derived absorption of culture liquids around 217 nm increases (Fig. S6b, inset). This reciprocal dependence of the absorbance in the 217 nm peak on the strain metabolic activity has been considered as a good reason to ascribe the 217 nm peak to the absorption of phosphate residuals in the cultivation supernatant at the end of bacterial growth.

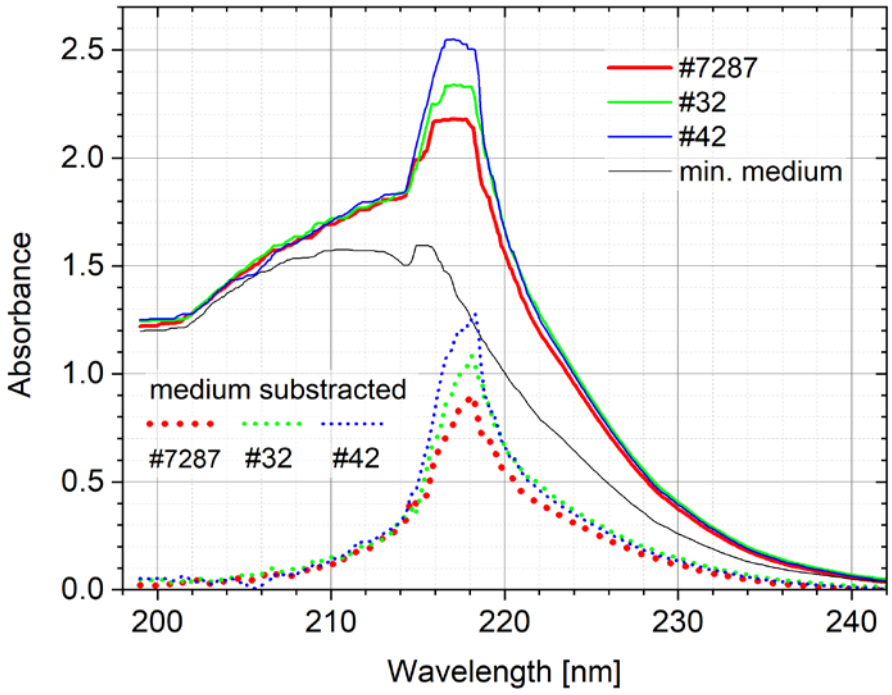

Figure S8: Absorption spectra of 64x diluted supernatant culture liquids (solid coloured) presented together with the absorption of 64x diluted MM medium (solid black) and results of its subtraction (doted coloured).

The normalized absorption spectra of culture supernatants with the initial 8 mM Na-Phy shows the difference in 250-310 nm range (Fig. S9) due to variation in the consumption of metal ions. Strain #42 consumes efficiently e.g., Mg^{2+} for pigment synthesis purpose [7], whereas culture liquids of strains #32 and #7287 reveal similar absorption profiles up to 300 nm belonging to the same group of soil *Bacillus megaterium* species. Strong increase in relative absorption at long-wavelength after 325 nm may be ascribed to the intensive synthesis of extracellular metabolites by strain #7287.

The revealed features and variation in the absorption spectra of Na-Phy solutions enabled us to suggest the following interpretation of absorption bands revealing the fate of Na-phytate upon its abiotic and biotic treatments. Absorption in 250-350 nm range is less pronounced in cold Na-Ph solution when the stabilizing Na^+ and PO_4^{3-} ligands are bound around inositol-ring of phytate molecule (Fig. S6a, blue). It is intensified due to the release of mobile ionic groups, i.e., when Na-Phy molecule is fragmented upon its autoclaving (Fig. S6b, red) or even during a long-term storage at 4°C. Thus, the absorption in complex broad bands within 250-350 nm range may be assigned to the interaction between cationic and anionic groups, e.g., oppositely charged Na^+ and PO_4^{3-} in case of Na-phytate solution [8].

Microbial cultivation experiment shows the correlation between the extent of PO_4^{3-} release and the trend in the absorption peak around 217 nm (Fig. S6b inset) supporting it assignment to orthophosphate ions released from Na-Phy. The data firstly demonstrate Na-Phy spectrum modification after enzymatic microbial degradation. Sodium is very wide spred in soils and Na-Phy is easier accessable to microorganisms than heavy metal phytate salts, which are low soluble or

insoluble. When phytate binds metals such as Cu^{2+}, Zn^{2+}, or Sr^{2+}, new absorption bands appear, for example a strong band in roughly 150-300 nm assigned to charge-transfer transitions between phosphate groups and the metal, plus weaker d-d bands in the visible region [1, 9].

The revealed trends in absorption spectra of phytate-containing solution may be employed for qualitative studies of phytate conversion in soil involving microbial activity. For this purpose, soil extracts have to be considerably diluted but may still introduce too broad variety of salt ionic groups making the absorption spectra too complex and difficult to interpret.

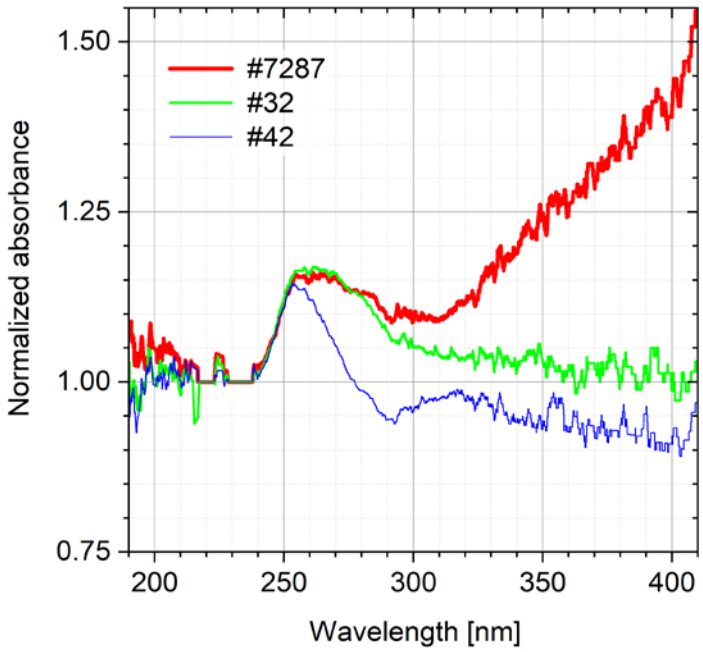

Figure S9: Absorption spectra of supernatant culture liquid with initial 8 mM Na-phy after growth of phytase-active bacterial strains.

References

1. Marolt, G. and M. Kolar, *Analytical Methods for Determination of Phytic Acid and Other Inositol Phosphates: A Review.* Molecules, 2020. **26**(1).
2. Ur Rahman, S., et al., *Exploring the Functional Properties of Sodium Phytate Doped Polyaniline Nanofibers Modified FTO Electrodes for High-Performance Binder Free Symmetric Supercapacitors.* Polymers (Basel), 2021. **13**(14).
3. Li, Q., et al., *In-depth characterization of phytase-producing plant growth promotion bacteria isolated in alpine grassland of Qinghai-Tibetan Plateau.* Front Microbiol, 2022. **13**: p. 1019383.
4. Crea, F., et al., *Formation and stability of phytate complexes in solution.* Coordination Chemistry Reviews, 2008. **252**(10-11): p. 1108-1120.
5. Wang, H., et al., *Sodium Phytate Cross-Linked Polyacrylic Acid as Multifunctional Aqueous Binder Stabilizes LiNi0.8Co0.1Mn0.1O2 to 4.6 V.* ACS Energy Letters, 2025. **10**(1): p. 136-144.
6. May, A.M. and J.L. Dempsey, *A new era of LMCT: leveraging ligand-to-metal charge transfer excited states for photochemical reactions.* Chemical Science, 2024. **15**(18): p. 6661-6678.
7. Devi, M., et al., *Bacteria as a source of biopigments and their potential applications.* J Microbiol Methods, 2024. **219**: p. 106907.
8. Sun, M., Z. He, and D.P. Jaisi, *Role of metal complexation on the solubility and enzymatic hydrolysis of phytate.* PLoS One, 2021. **16**(8): p. e0255787.
9. Zajac, A., et al., *Spectroscopic properties and molecular structure of copper phytate complexes: IR, Raman, UV-Vis, EPR studies and DFT calculations.* J Biol Inorg Chem, 2019. **24**(1): p. 11-20.